159

[redacted]

Copy
RM L56H29a

5578

AUG 13 1957

TECH LIBRARY KAFB, NM

0144244

NACA RM L56H29a

7717

RESEARCH MEMORANDUM

DYNAMIC MODEL INVESTIGATION OF TWO TAIL-SITTER VERTICALLY RISING AIRPLANES TO DETERMINE THE ALTITUDE REQUIRED TO APPROACH NORMAL-FLIGHT CONDITIONS AFTER POWER FAILURE IN HOVERING FLIGHT

By Walter J. Klinar and L. Faye Wilkes

Langley Aeronautical Laboratory
Langley Field, Va.

[redacted]

NATIONAL ADVISORY COMMITTEE
FOR AERONAUTICS

WASHINGTON
November 9, 1956

[redacted]

TECH LIBRARY KAFB, NM
0144244

NATIONAL ADVISORY COMMITTEE FOR AERONAUTICS

RESEARCH MEMORANDUM

DYNAMIC MODEL INVESTIGATION OF TWO TAIL-SITTER VERTICALLY RISING AIRPLANES TO DETERMINE THE ALTITUDE REQUIRED TO APPROACH NORMAL-FLIGHT CONDITIONS AFTER POWER FAILURE IN HOVERING FLIGHT

By Walter J. Klinar and L. Faye Wilkes

SUMMARY

An investigation has been undertaken on two dynamic models simulating 1/20-scale and 1/25-scale models of propeller-driven tail-sitter vertically rising airplanes to determine the altitude required to approach normal-flight conditions after power failure in hovering flight. The results of the investigation indicated that, for the two models investigated, an altitude of 3,600 to 5,400 feet may be required to attain normal gliding flight.

INTRODUCTION

A problem of concern to designers of vertical-take-off-and-landing (herein designated VTOL) airplanes has been the determination of the altitude required by such an airplane to make a belly landing after power failure during hovering flight. Associated with this problem is the altitude requirement for such airplanes to turn over and nose down into the direction of flight after power failure. Accordingly, an investigation was undertaken with dynamic models of two propeller-driven tail-sitter VTOL airplanes to provide some information on this latter problem. These tests were conducted in the free-flying area of the Langley spin-tunnel building. Simplified calculations were also made to project the flights beyond that which could be observed in the test area. The results of the investigation are presented herein.

[redacted]

[redacted]

SYMBOLS

A sketch depicting the positive directions of various angles, velocities, and forces is shown in figure 1.

b	wing span, ft
S	wing area, sq ft
$\bar{c}$	mean aerodynamic chord, ft
$x/\bar{c}$	ratio of distance of center of gravity rearward of leading edge of mean aerodynamic chord to mean aerodynamic chord
$z/\bar{c}$	ratio of distance between center of gravity and fuselage reference line to mean aerodynamic chord (positive when center of gravity is below line)
m	mass of airplane, slugs
I_X, I_Y, I_Z	moments of inertia about X, Y, and Z body axes, respectively, slug-ft^2
$\frac{I_X - I_Y}{mb^2}$	inertia yawing-moment parameter
$\frac{I_Y - I_Z}{mb^2}$	inertia rolling-moment parameter
$\frac{I_Z - I_X}{mb^2}$	inertia pitching-moment parameter
ρ	air density, slug/cu ft
μ	relative density of airplane, $\frac{m}{\rho S b}$
α	angle between fuselage reference line and the relative wind, deg (See fig. 1.)
t	full-scale time, sec
V_R	full-scale resultant velocity, ft/sec (See fig. 1.)

V_Z full-scale sinking speed, ft/sec (See fig. 1.)

g acceleration due to gravity, 32.2 ft/sec^2

γ flight-path angle, deg (See fig. 1.)

Z altitude loss, ft

L lift, lb (See fig. 1.)

D drag, lb (See fig. 1.)

C_D drag coefficient, $\frac{D}{\frac{1}{2}\rho V_R^2 S}$

C_L lift coefficient, $\frac{L}{\frac{1}{2}\rho V_R^2 S}$

δ_e elevon deflection when deflected as elevators (positive with trailing edge down), deg

$\dot{V}_R$ rate of change of velocity V_R with time

$\dot{\gamma}$ rate of change of flight-path angle with time

β simulated propeller blade angle, deg

APPARATUS AND METHODS

Model

Model 1 was assumed to be a 1/20-scale model of a swept-wing VTOL airplane and model 2 was considered representative of a 1/25-scale straight-wing VTOL airplane. Fixed area was attached to each model to simulate propellers. Three-view drawings of the models used in the investigation are shown in figures 2 and 3. Dimensional characteristics of the airplanes as simulated by the model are presented in table I. Model 2 was ballasted to obtain dynamic similarity to the corresponding airplane at sea level (ρ = 0.002378) whereas model 1 was ballasted as close to sea level as was possible on the model, this latter condition corresponded to an altitude of 5,000 feet (ρ = 0.002049). The differences in these altitude effects are considered to be insignificant.

[redacted]

Testing technique.- The tests were performed in a large building at Langley. The models were attached to a device from which they could be released after being hoisted to the top of the building. After release the models had available approximately 50 feet of free fall after which they dived into a safety net. Motion-picture records were made of the various drop tests. Model attitudes could be determined from some of these tests when the model was properly oriented with respect to the camera.

Computations.- Brief computations were made to determine the motion that ensued after the models dropped vertically for the height available in the test area. In order to simplify the problem it was assumed that the paths of the models' motions could be approximated by neglecting the pitching equation. The angle of attack was assumed to be constant during this part of the flight; thus, any variation in angle of attack was assumed to be instantly corrected. The equations used were as follows:

$$\dot{V}_R = g \sin \gamma - \frac{\rho S C_D}{2m} V_R^2$$

$$-\dot{\gamma} = \frac{\rho S C_L}{2m} V_R - \frac{g \cos \gamma}{V_R}$$

These equations were solved with the Runge-Kutta method and the lift and drag coefficients, angle of attack, and elevator position were taken as follows:

Model	α, deg	δ_e, deg	C_L	C_D
1	30	-30	0.85	0.60
2	12	-16	.70	.30

Test Conditions

The models were tested for the loading conditions indicated in table II. Model 1 which had a 30° propeller blade angle simulated by the addition of fixed fin area to the nose of the model was dropped from a nose-up attitude and also from several different initial attitudes. Model 2 was dropped only from a nose-up attitude either without propellers simulated or with fixed fin area added to the nose to simulate a 15° or 70° propeller blade angle. On both models, the lateral and directional controls were maintained at neutral. On model 1 the elevator was maintained at its full-up deflection of -30°, and on model 2 the elevons were also maintained full-up at -16°.

RESULTS AND DISCUSSION

The results of the tests are presented in full-scale terms in figures 4 and 5. These results indicate that neither model tumbled for the center-of-gravity positions investigated. As is indicated in figure 4 for model 1 the most critical launching attitude as regards altitude loss before the model turned over and nosed into the direction of the relative wind was from a nose-up attitude. The model test results indicate that, when launched from a nose-up attitude, approximately 550 feet of altitude was required for model 1 and approximately 750 feet for model 2 (full-scale values) to assume nose-first attitudes. The slight differences in the flights presented in figure 5 for model 2 are considered to be attributable to different launchings rather than to differences in propeller fin area simulated. The flight paths of the models for the various drops were observed to be nearly vertical for the height available and the average acceleration during the various drops was approximately the acceleration due to gravity as is indicated by the time and altitude scales in figures 4 and 5.

The results of computations made to obtain an approximation of the projected flight paths beyond that observable by the model tests are presented in figures 6 and 7. These calculations were made to extend those flights when the models were dropped from a nose-up attitude with the elevator maintained full up. To obtain the initial velocities for these computations, the models were assumed to accelerate uniformly during the observed drop period in the test area. The trim values indicated on figures 6 and 7 are for the trimmed glide conditions. The computations indicate that a considerable amount of altitude may be required for designs similar to the ones under consideration to make a belly landing after power failure while hovering. In order to reach minimum points in the glide-path angle, at which time the fuselages of the two designs were approximately horizontal, the calculations indicated the full-scale values of approximately 3,600 feet and 5,400 feet would be required for models 1 and 2, respectively. In order to obtain a horizontal glide path apparently the elevator would have to be moved from its full-up position to obtain a speed build up after the models assumed nose-down attitudes. It is felt that altitudes of the order obtained would have been required had such cases been considered.

CONCLUSIONS

Results of free-drop tests of dynamic models of two airplanes which take off and land vertically indicated that the full-scale altitude required for the designs to turn over and nose into the relative wind after power failure during hovering flight corresponded to approximately

550 feet for one of the designs and 750 feet for the other design (full-scale values). Approximate computations to extend the flight paths beyond that which could be observed in the tests indicated that as much as 3,600 to 5,400 feet (full-scale) may be required for the corresponding airplanes to attain normal gliding flight.

Langley Aeronautical Laboratory,
National Advisory Committee for Aeronautics,
Langley Field, Va., August 15, 1956.

TABLE I.- DIMENSIONAL CHARACTERISTICS OF THE AIRPLANES AS SIMULATED ON MODELS

	Model 1	Model 2
Overall length, ft	32.18	37.5
Wing:		
Span (not including pods), ft	25.67	27.5
Area, sq ft	346	246
Airfoil section	NACA 63009	Modified NACA 64A206
Mean aerodynamic chord, in.	186.9	116.5
Leading edge $\bar{c}$ behind wing apex, in.	85.20	18.175
Tip chord, in.	52.00	5.3
Root chord, in.	272.00	162
Incidence, deg	0	1
Dihedral, deg	0	5
Taper ratio	0.191	0.327
Effective aspect ratio	1.9	3
Distance from normal center of gravity to intersection of elevon hinge line and fuselage center line, in.	134.6	----------
Distance from normal center of gravity to intersection of rudder hinge line and fuselage center line, in.	135.0	----------
Sweepback of leading edge of wing, deg	55.0	----------
Sweepback of trailing edge of wing, deg	0	----------
Distance from the center of gravity for the take-off loading (with fuel and ammunition) to intersection of control hinge line and fuselage center line, in.	----------	178.80
Elevons:		
Exposed span of one elevon, ft	10.02	----------
Chord behind hinge line (constant), in.	21.80	----------
Exposed area of elevon rearward of hinge line (total), sq ft	36.2	----------
Vertical tail:		
Span, overall, ft	22.97	----------
Total area, sq ft	160.5	----------
Rudder area rearward of hinge line, sq ft	20.75	----------
Sweepback of leading edge of fin, deg	40.0	----------
Sweepback of trailing edge of fin, deg	3.0	----------
Tail surfaces:		
Span, ft	----------	12.25
Total area, sq ft	----------	169
Area - 4 fixed surfaces, sq ft	----------	136.2
Area - movable surfaces, sq ft	----------	32.8
Airfoil section	----------	NACA 65A007
Incidence, deg	----------	-4

TABLE II.- MASS CHARACTERISTICS AND INERTIA PARAMETERS FOR MODELS 1 AND 2

[Model values converted to full-scale values; moments of inertia are about the center of gravity]

Model	Loading	Weight, lb	Center-of-gravity location		Relative density, μ		Moments of inertia, slug-feet^2			Mass parameters		
			$x/\bar{c}$	$z/\bar{c}$	Sea level	Altitude of 5,000 ft	I_X	I_Y	I_Z	$\frac{I_X - I_Y}{mb^2}$	$\frac{I_Y - I_Z}{mb^2}$	$\frac{I_Z - I_X}{mb^2}$
1	Full load gross weight	16,306	0.159	-0.012	23.98	27.82	12,507	24,348	32,905	-355×10^{-4}	-256×10^{-4}	611×10^{-4}
2	Take-off heavy loading	16,200	0.053	0.029	31.27	--	8,895	36,044	41,105	-714×10^{-4}	-133×10^{-4}	847×10^{-4}

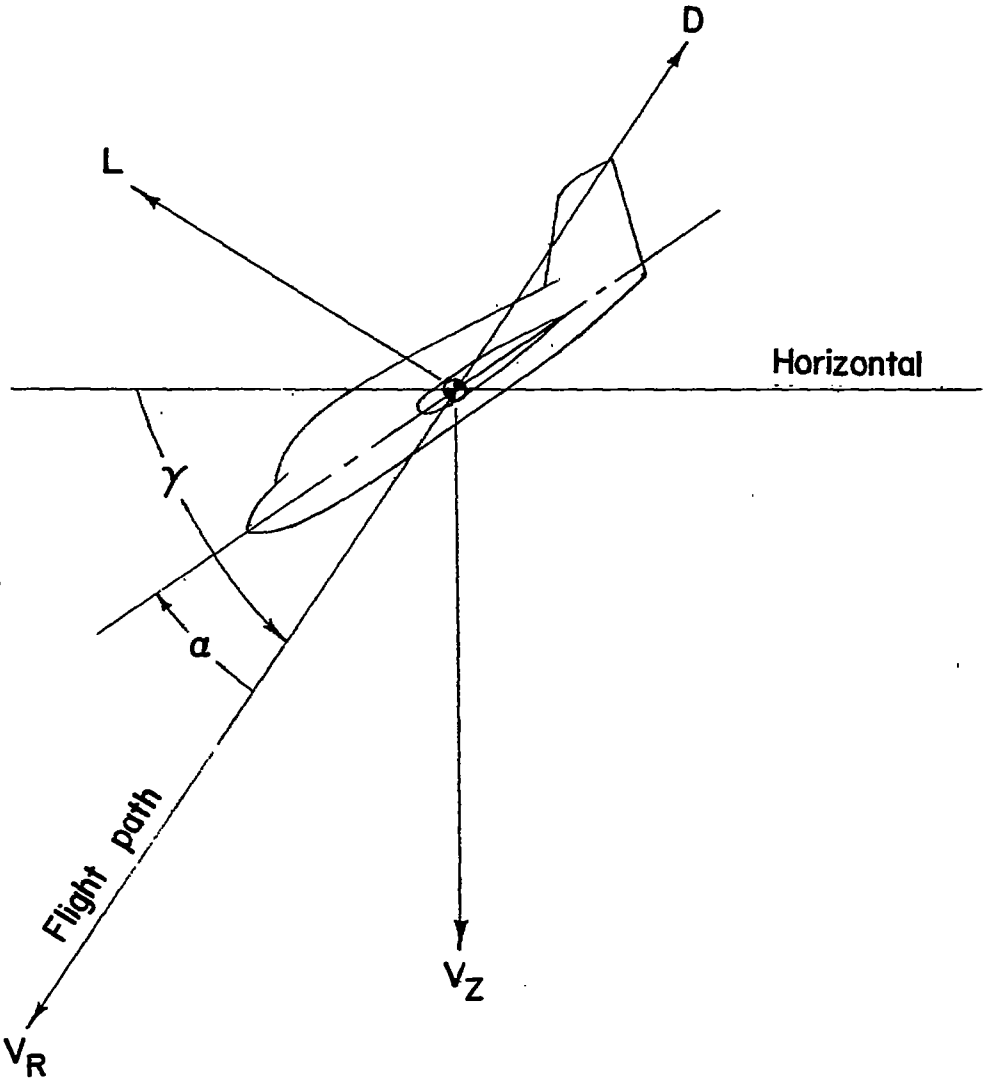

Figure 1.- Illustration depicting positive forces, velocities, and angles.

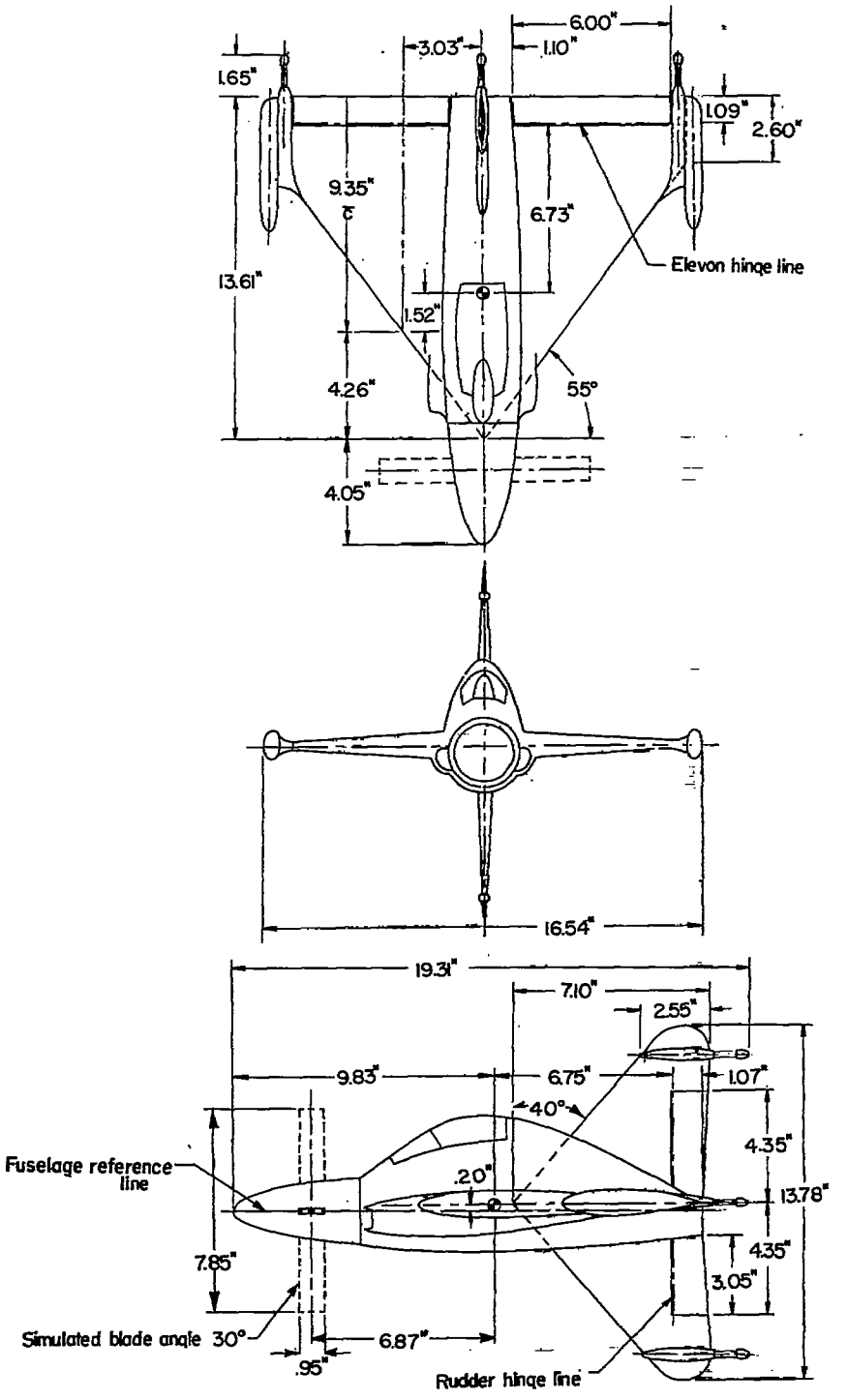

Figure 2.- Three-view drawing of model 1. (Dimensions are model values.)

[redacted]

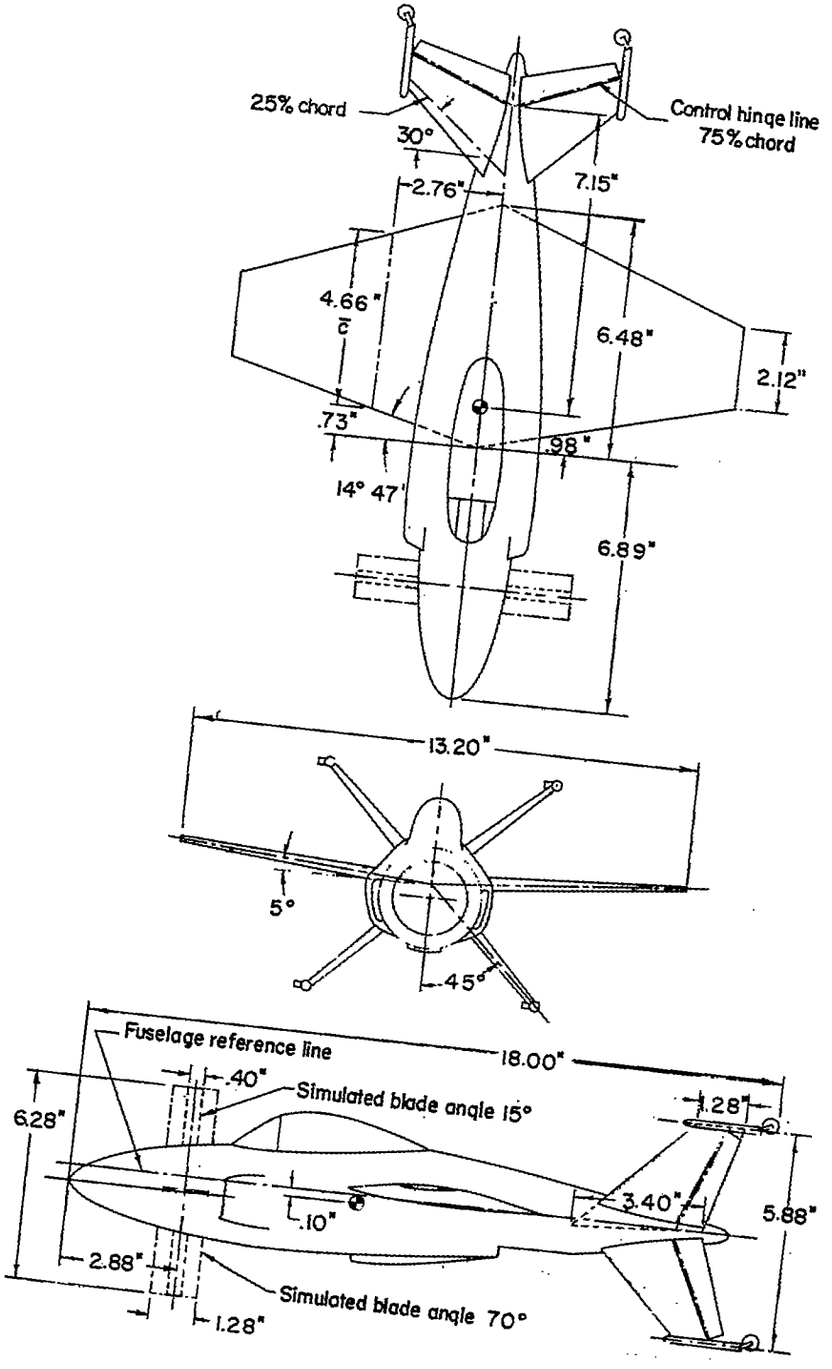

Figure 3.- Three-view drawing of model 2. (Dimensions are model values.)

[redacted]

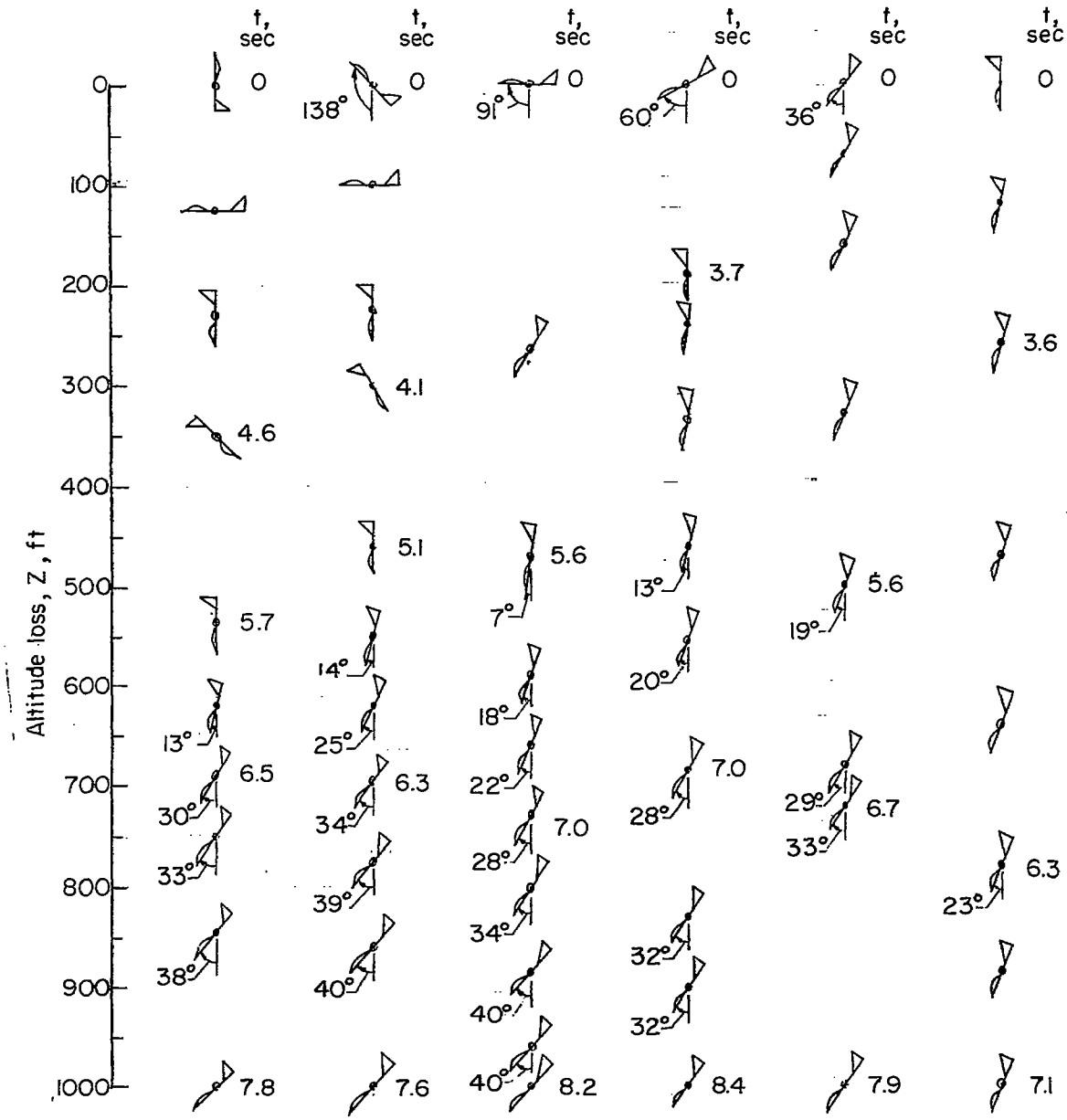

Figure 4.- Typical motions of model 1 when dropped from various attitudes. Propeller blade angle of 30° simulated. (Angles of attack given are approximate; values are given in full-scale terms.)

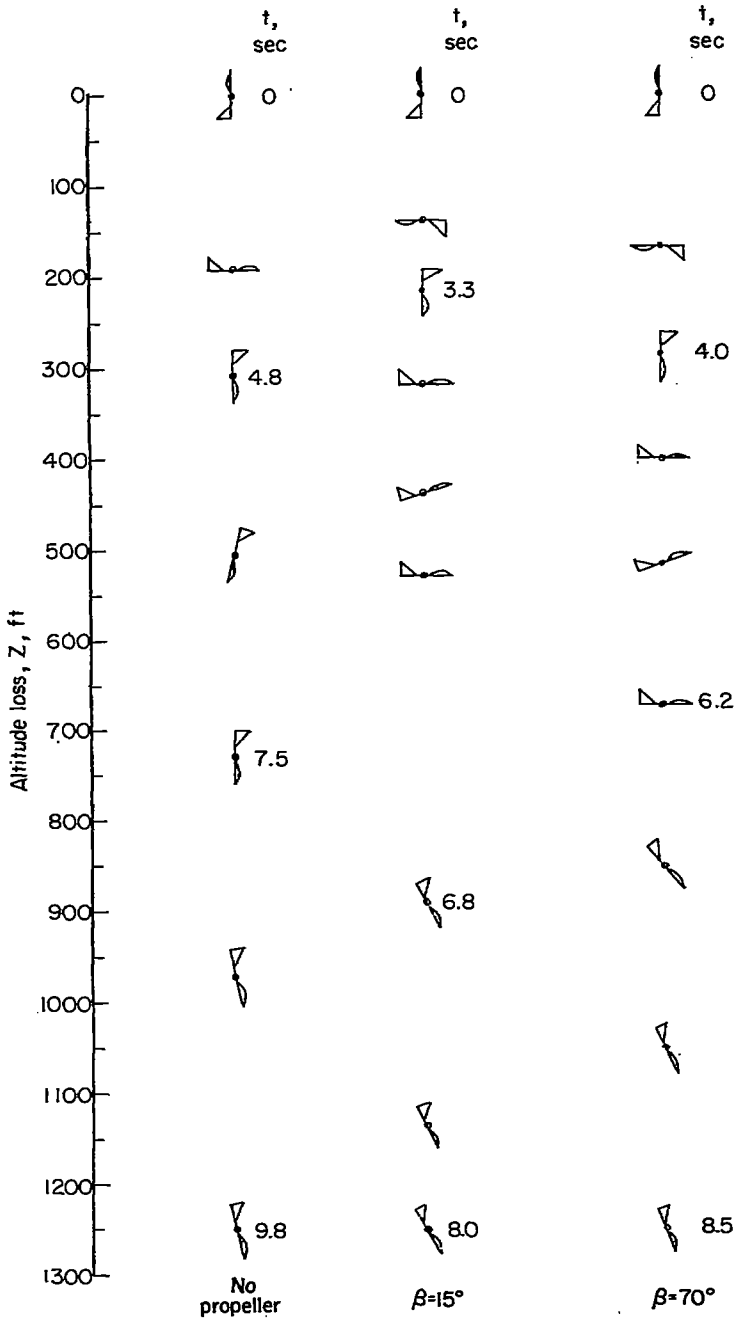

Figure 5.- Typical motions of model 2 when dropped from nose-up attitude. (Values are given in full-scale terms.)

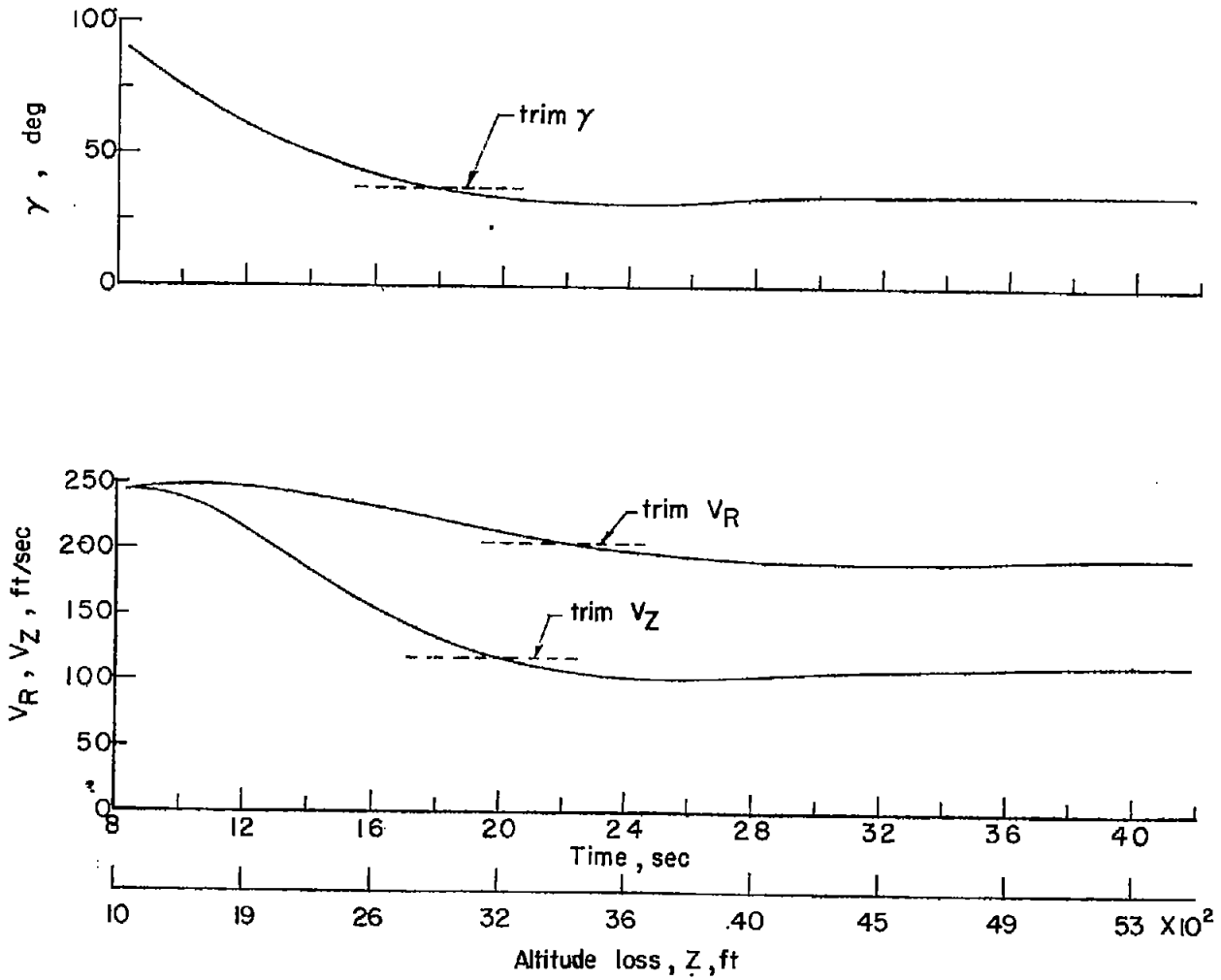

Figure 6.- Calculated motion for model 1 projected beyond the motion observed in the free-drop tests. (Values are given in full-scale terms.)

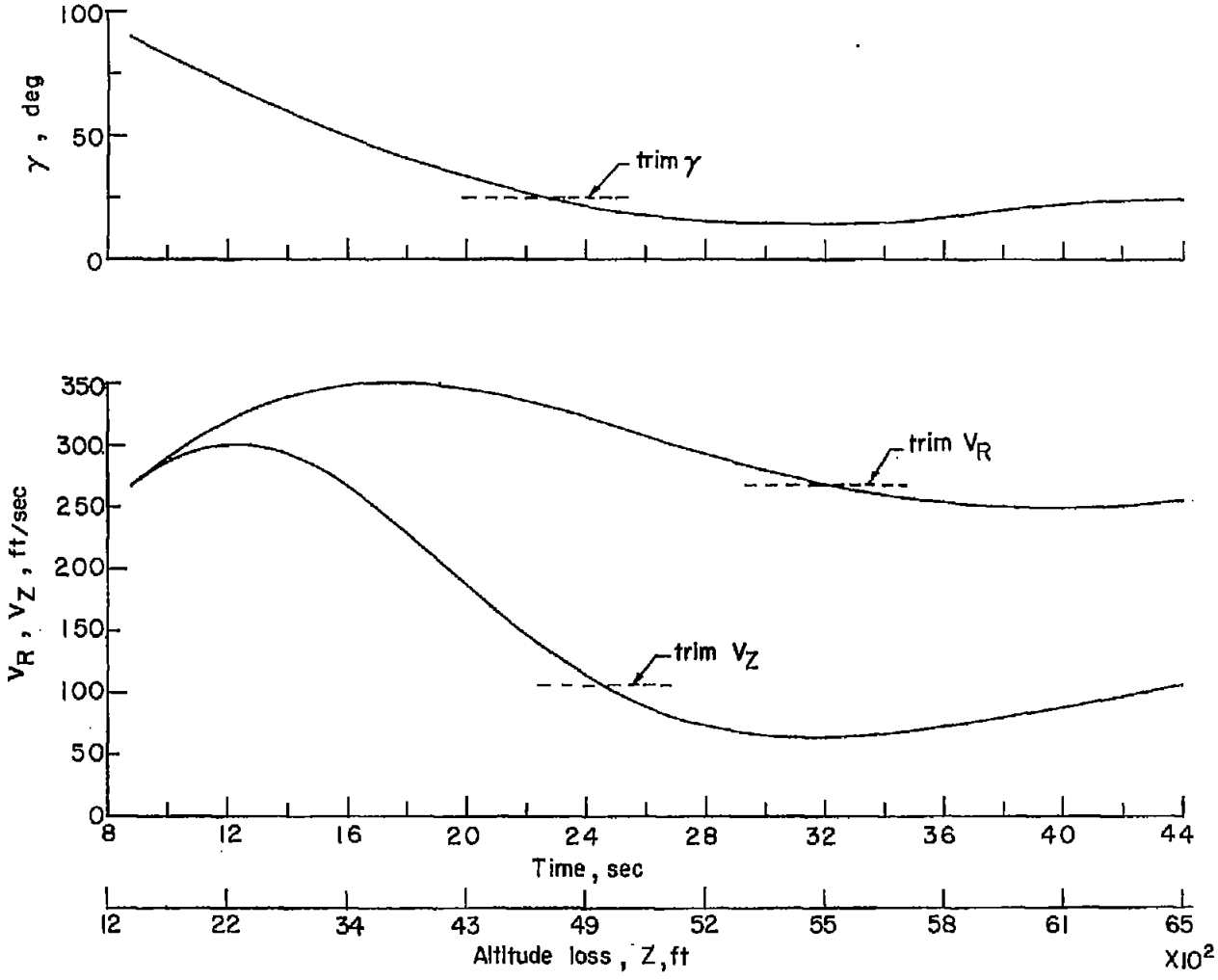

Figure 7.- Calculated motion for model 2 projected beyond the motion observed in the free-drop tests. (Values are given in full-scale terms.)